9th International Congress of the Serbian Society of Mechanics
July 5-7, 2023, Vrnjačka Banja, Serbia

ANALYTICAL DESIGN OF RESONANT CONTROLLER APPLIED FOR SOLVING ROBOT ARM TRACKING PROBLEM

Petar D. Mandić[1], Tomislav B. Šekara[2], Mihailo P. Lazarević[1]
[1] University of Belgrade,
Faculty of Mechanical Engineering, Kraljice Marije 16, Belgrade 11120, Serbia
e-mail: pmandic@mas.bg.ac.rs, mlazarevic@mas.bg.ac.rs
[2] University of Belgrade,
School of Electrical Engineering Bulevar kralja Aleksandra 73, Belgrade 11120, Serbia
e-mail: tomi@etf.rs

Abstract:

This paper deals with a topic of robot following a trajectory in three-dimensional space with a prescribed velocity law. Considering the nonlinear nature of robot manipulators, and high demands regarding tracking performances, this task is very challenging, but also very popular in control community because of its importance in industrial applications. To tackle successfully this problem, we proposed a resonant controller, which outperforms classical control schemes usually employed in this situation. In this particular case, the robot manipulator needs to follow an ellipse trajectory with constant speed along the curve. First, mathematical model of the three degrees of freedom robot arm is derived with included actuator dynamics. Then, numerical solution of inverse kinematics problem needs to be calculated in order to obtain desired trajectory in joint space. Third, analytical procedure for designing a resonant controller is given, with parameters of the controller chosen in order to achieve a good performance/robustness trade-off, which is a key element in modern control design. Finally, the proposed control scheme is tested and results of robot simulation are given at the end. Final remarks conclude the paper.

Key words: robot trajectory control, resonant controller, robust control, inverse kinematics

1. Introduction

Robotics is a multidisciplinary field wherein knowledge of several different disciplines like electrical, mechanical and systems engineering are needed in order to successfully cope with it. Also, advances in computer science are main cause of rapid development of robotics over the past decades [1]. Majority of robot applications deal within industrial conditions, executing tasks such as welding, packaging, cutting, paint spraying, moving objects etc. Industrial manipulators need to fulfill high demands in terms of accuracy, precision and repeatability. One of such typical applications is a task of following a trajectory in space with prescribed velocity law.

Designing a controller for such a task is not so straightforward. Scientific community reports a large number of different control strategies for robotic manipulators [2]. Most of them are based on linear control theory from a practical reason. Namely, linear controllers are intuitive, easy to understand and last but not least, easy to implement. This approach gains even more importance when robot dynamics can be regarded as linear, which can be achieved by using motors with high gear ratios, or by using feedback linearization techniques. This way, dynamic coupling effects can be neglected and control of each robotic joint can be designed independently. This is the reason why classical PID controllers are still an inevitable part of control of robot manipulators in industry [3-9].

Besides classical control strategies, improving performances of the closed loop system can be achieved by applying a bit more complex algorithms such as resonant controllers [10]. These regulators are capable of tracking sinusoidal references (with or without offsets) of arbitrary frequencies with zero steady state error, and they achieve it while preserving good transient response [11]. They have been applied successfully in cases such as alternate current systems, wind turbines, active rectifiers, motor drives etc [12,13].

Having in mind given task of robot following desired path, resonant controller proposed in this paper imposes as a reasonable choice. Namely, following closed trajectory in space with constant speed several times in a row is a repetitive task for robot manipulator, meaning that robot joints need to track complex periodic signals with the same fundamental frequency. In order to do so, several steps need to be resolved successfully. Deriving a mathematical model of robot manipulator with the actuator dynamics is a first one. Then, solving an inverse kinematics problem is necessary in order to obtain desired trajectories in joint space. Design of a robust controller with good closed loop system performances is the next important step. Finally, simulation of the robot performing the abovementioned task is necessary to validate the effectiveness of the proposed procedure. All these steps will be described in more detail in following sections.

2. Mathematical model of robotic manipulator and solution of the inverse kinematics problem

The mechanical structure of robot arm can be described as a sequence of rigid bodies interconnected by means of joints. Dynamic equations of the robotic system can be written in the following form [14]:

$$A(\boldsymbol{q})\ddot{\boldsymbol{q}} + C(\boldsymbol{q},\dot{\boldsymbol{q}})\dot{\boldsymbol{q}} - \boldsymbol{Q}^{g} = \boldsymbol{Q}^{m}, \tag{1}$$

wherein: $\boldsymbol{q}(t) \in R^3$ is the vector of the generalized coordinates, $A(\boldsymbol{q}) \in R^{3\times 3}$ represents basic metric tensor (or inertia matrix), $C(\boldsymbol{q},\dot{\boldsymbol{q}}) \in R^{3\times 3}$ is a matrix that includes centrifugal and Coriolis effects, $\boldsymbol{Q}^{g} \in R^3$ and $\boldsymbol{Q}^{m} \in R^3$ are gravity term and torque vectors applied to the joints, respectively. For details of the calculation of the basic metric tensor and matrix $C(\boldsymbol{q},\dot{\boldsymbol{q}})$ for robot manipulators, the reader is referred to [15].

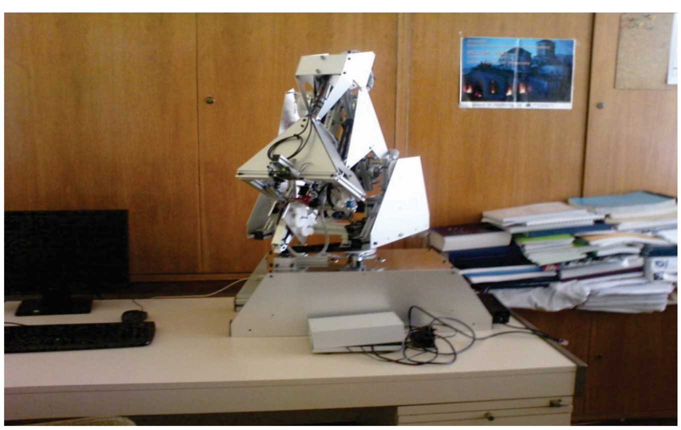

Fig. 1. Robotic manipulator with seven DOFs

In this paper we considered a robotic system which is an integral part of the Laboratory of Applied Mechanics at the Faculty of Mechanical Engineering in Belgrade (Figure 1). It has seven degrees of freedom (DOFs), but only the first three revolute joints are responsible for placing the end-effector into the demanded position in space [16]. The following three DOFs are in the form of the spherical wrist and they are responsible for end-effector's orientation. The 7th DOF is the gripper. Herein, robot arm with first three revolute joints is considered since these robot links are engaged in tracking the desired path in space.

Usually, robot links are driven by DC motors. Since motor's optimal working condition include high angular speeds, while controlling the movement of robot link demands low speeds [17], it is necessary to interpose a gear transmission between motors and joints. If N represents diagonal matrix of the gear ratios, the following equations describe connection between motors and robot links:

$$\boldsymbol{q}_m = N\boldsymbol{q},\ \ \boldsymbol{Q}^{\boldsymbol{m}} = N\tau_l, \tag{2}$$

wherein $\boldsymbol{q}_m$ represents the positions of the actuators shafts, while τ_l is the vector of torques resulting from the robot manipulator and acting on the motors shafts. It can be easily shown [18] that torque τ_l is equal to:

$$\tau_l = \left(N^2\right)^{-1}\left(A(\boldsymbol{q})\ddot{\boldsymbol{q}}_m + C(\boldsymbol{q},\dot{\boldsymbol{q}})\dot{\boldsymbol{q}}_m\right) - N^{-1}\boldsymbol{Q}^g \tag{3}$$

Torque τ_l can be described as a disturbance acting on the motor shafts. The influence of this disturbance on motor's dynamics decreases with the increase of the reduction ratio N. Consequently, it means that the presence of large reduction ratio tends to linearize the dynamic equations of robot. This allows us to introduce a major simplification in our mathematical model. Instead of nonlinear dynamic equations of robot given by (1), we can use linear model of DC motor instead.

Robot manipulator from the above picture uses three identical Maxon DC motors for controlling the position of the first three links. The transfer function $G_m(s)$ of these motors can be described as:

$$G_{\mathrm{m}}(s) = \frac{K}{s(Ts+1)}. \tag{4}$$

wherein K=22.515 and $T = 0.0056409$. Finally, to sum up, the original nonlinear robotic system, due to high reduction ratio $\left(N = \mathrm{diag}\{185,632,140\}\right)$ can be represented by 3 linear, decoupled subsystems, using the motor transfer function $G_{\mathrm{m}}(s)$.

2.1 Inverse kinematics problem

The inverse kinematics problem consists of the determination of the joint variables corresponding to a given end-effector position. As mentioned before, tip of the robot arm needs to follow an ellipse curve with constant speed along the path. In this example, ellipse lies in a plane parallel to the referential horizontal plane, with value of 0.2m corresponding to the semi-major axis, and 0,1m for the semi-minor axis. Desired end-effector speed along the path is 0.2m/s. Before tackling with the inverse kinematics, coordinates of the robot tip with respect to the inertial reference frame need to be calculated. This is achieved by applying numerical procedures, since an analytical solution is not possible in this case. Graphical representations of equations of motion of the robot tip obtained in Cartesian coordinates are depicted in Figure 2.

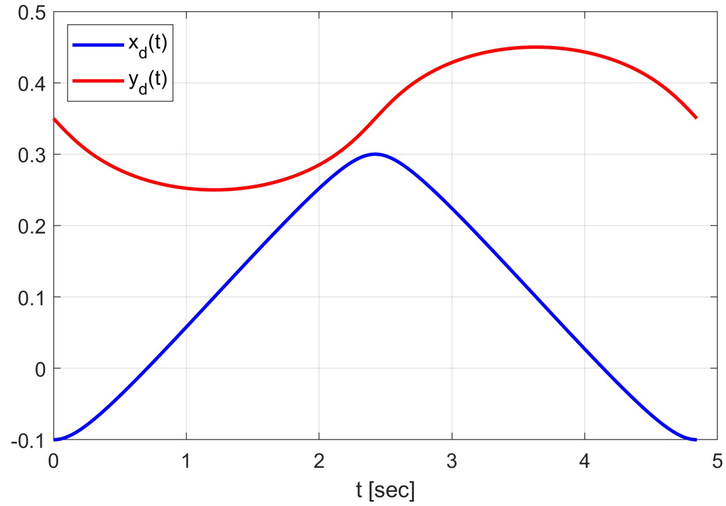

Fig. 2. Cartesian coordinates of reference trajectory

Now, knowing the position of end-effector with respect to inertial frame at every time instance, we can determine desired values of joint variables $\boldsymbol{q}_d$. In this case, for the given robot configuration, analytical solution is possible and is graphically illustrated in Figure 3. For more details about solving inverse kinematics problem, the reader is referred to [19,20].

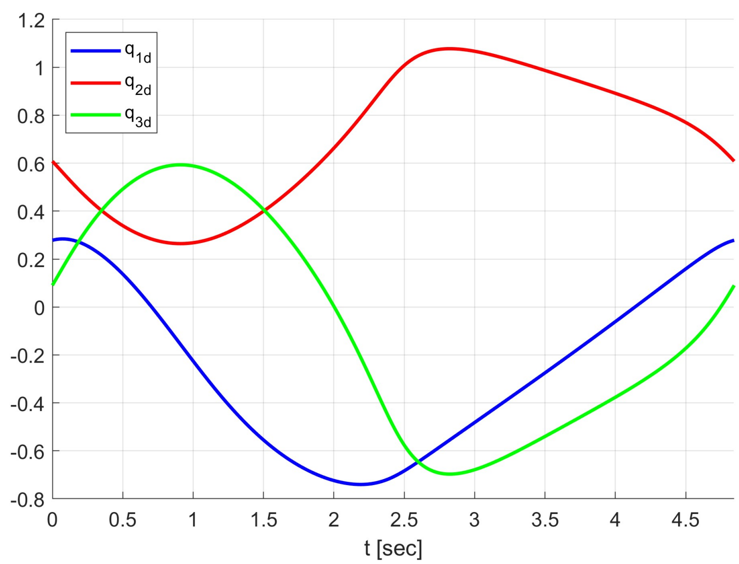

Fig. 3. Graphical solution of inverse kinematics problem

Here, we should notice that the oscillatory period is approx. 4,85 seconds, which corresponds to the value of natural frequency $\omega_0 \approx 1,295\ \mathrm{s}^{-1}$.

3. Controller design

The control scheme of the closed loop system is depicted in Figure 4, where $G_\mathrm{m}(s)$ is model of motor given by (4), $C(s)$ is the employed controller, while *r*, *d*, *u* and *y* represent reference, disturbance, control and output signal, respectively.

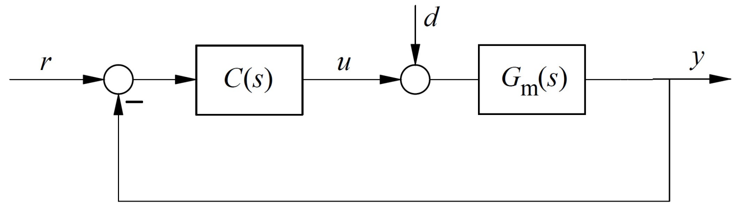

Fig. 4. Block diagram of closed loop control system

In this paper, parameters of the resonant controller $C(s)$ are derived specifically for the plant $G_{\mathrm{m}}(s)$, but described procedure can be applied to any other plant model [21]. To begin with, we start with the complementary transfer function $T(s)$ given by [22,23]:

$$T(s) = \frac{\eta_4 s^4 + \eta_3 s^3 + \eta_2 s^2 + \eta_1 s + 1}{(\lambda s + 1)^2 (Ts + 1)^4} \tag{5}$$

where time constant $\lambda > 0$, and η_4, η_3, η_2 and η_1 are free parameters which will be determined to obtain the desired dynamic characteristics of the closed loop system. Having in mind that $T(s)$ can be formulated also as $T(s) = C(s)G_m(s) / (1 + C(s)G_m(s))$, then after some calculations, one obtains controller $C(s)$ in the following form:

$$C(s) = \frac{\eta_4 s^4 + \eta_3 s^3 + \eta_2 s^2 + \eta_1 s + 1}{(\lambda s + 1)^2 (Ts + 1)^4 - \eta_4 s^4 - \eta_3 s^3 - \eta_2 s^2 - \eta_1 s - 1} \frac{1}{G_m(s)}, \tag{6}$$

Free parameters η_4, η_3, η_2 and η_1 are determined in order to cancel the poles of $G_{\mathrm{m}}(s)$ and the poles of the controller: $s = 0$, $s_{1,2} = \pm i\omega_0$. Applying these conditions, we obtain:

$$\begin{aligned}
\eta_1 &= 2\lambda + 4T, \\
\eta_2 &= -2T^3\lambda\omega_0^2 \,\hat{}\, 2 - 3T^2\lambda^2\omega_0^2 + 6T^2 + 8T\lambda + \lambda^2, \\
\eta_3 &= -2T\left(T^3\lambda\omega_0^2 + 2T^2\lambda^2\omega_0^2 - 2T^2 - 6T\lambda - 2\lambda^2\right), \\
\eta_4 &= -T^4\lambda^2\omega_0^2 + T^4 + 6T^3\lambda + 3T^2\lambda^2
\end{aligned} \tag{7}$$

Substituting expressions from (7) into (6) we obtain $C(s)$ as a function of one tuning parameter λ:

$$C(s) = \frac{(Ts+1)\left(1 + T((1-\lambda^2\omega_0^2)T^2 + 6T\lambda + 3\lambda^2)s^3 + (-2T^3\lambda\omega_0^2 + (3-3\lambda^2\omega_0^2)T^2 + 6T\lambda + \lambda^2)s^2 + (3T + 2\lambda)s\right)}{sK(s^2 + \omega_0^2)(T\lambda s + 2T + 3\lambda)T^2\lambda} \tag{8}$$

By adjusting λ one can obtain very good robustness/performance trade-off, which is a key issue in modern control system design. Robustness with respect to modelling uncertainties is ensured by constraining the largest value of the sensitivity function $M_{\mathrm{s}} = \max_{\omega} |1 - T(i\omega)|$. Sensitivity to model uncertainties can also be expressed with the largest value of the complementary sensitivity function $M_{\mathrm{p}} = \max_{\omega} |\mathrm{T}(i\omega)|$. The sensitivity to measurement noise M_{n} is defined as $M_{\mathrm{n}} = \max_{\omega} |C(i\omega) / (1 + C(i\omega)G_m(i\omega))|$.

The reader should observe the term $s^2+\omega_0^2$ in the denominator of the above expression. While this term is capable of tracking fundamental frequency ω_0 of periodic signal $\boldsymbol{q}_d$, another pole $s=0$ of the controller is responsible for bringing the offset of $\boldsymbol{q}_d$ to zero steady state error.

4. Simulation results

To validate performance of the resonant controller given by (8), simulation of robotic manipulator executing the given task is performed [24]. Choosing $\lambda = 10T \approx 0.056409$, a very good compromise between robustness and performance is obtained $\left(M_s \approx 1.36,\ M_{\mathrm{p}} \approx 1.48\right)$, in which case transfer function of resonant controller equals to:

$$C(s)=\frac{29.368(s+15.620)(s+27.620)(s+39.455)(s+183.161)}{s(s+586.116)(s^2+1.677)} \tag{9}$$

Controller (9) written in above form is not suitable for practical realization. In order to be implemented in real time application, one should perform partial fraction decomposition of given transfer function to obtain:

$$C(s)=\frac{93149.09}{s}+\frac{29.368s+6976.05}{s+586.1162704}+\frac{-92317.59s+20182.47}{s^2+1.677} \tag{10}$$

Now, resonant controller can be realized in parallel series according to (10). Regarding simulation, robot arm is programmed to follow ellipse curve several times in a row. Results of the simulation are depicted in Figure 5.

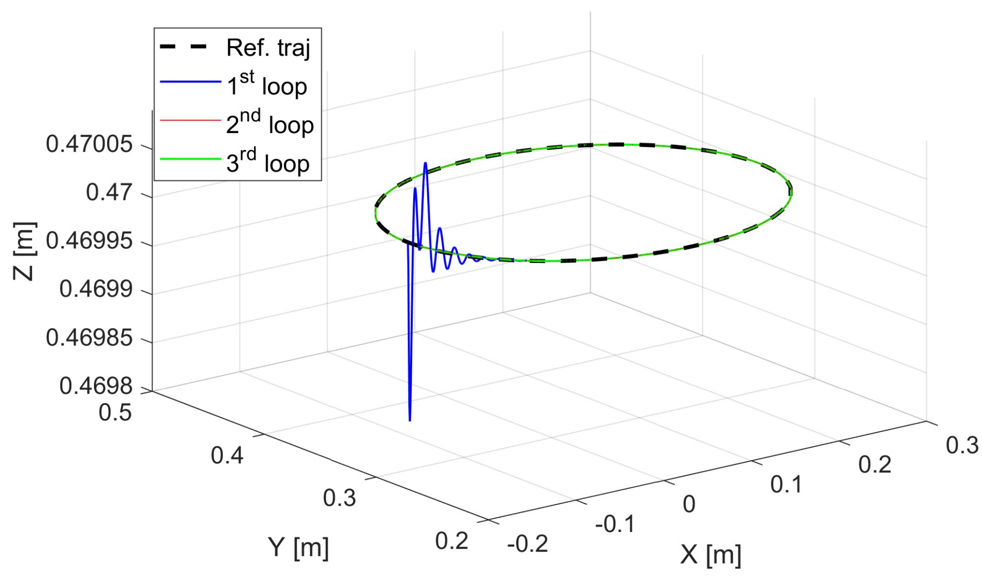

Fig. 5. Comparison between reference and actual trajectories for different loops

As a measure of tracking performance, maximum absolute error between actual and reference path is calculated after every loop. Results are summarized in table below. We can see the biggest error occurred during the first loop, which is expected due to initial conditions mismatch. During the second loop error decreased significantly, and remained stable in the following iterations. Similar conclusions can be derived by observing trajectories in Figure 5.

Loop No.	1	2	3	4, 5 etc.
Max. error [mm]	5,408e^{-01}	1,3606e^{-02}	1,3606e^{-02}	1,3606e^{-02}

Table 1. Evolution of maximum absolute error (in milimeters)

At the end, it is worth saying that the tracking error would be even smaller if we chose to track not only fundamental frequency ω_0, but also higher harmonics of periodic signal $\boldsymbol{q}_d$. Analytical procedure described above for the design of resonant controller could be employed with insignificant changes, but in that case the price would be paid in terms of complexity of the regulator, which would be of higher degree.

5. Conclusion

In this paper a resonant controller is employed for executing robots' repetitive tasks. In order to do it successfully several steps need to be overcome. Mathematical model of robot is derived, followed by an inverse kinematics problem solution. Resonant controller is designed analytically as a function of one adjustable parameter. Choosing λ appropriately a good compromise between robustness and system performance is obtained. Simulation of robot following a desired ellipse curve in space shows effectiveness of the proposed controller. Designed procedure can be generalized for different type of plants, but also for different end-effectors' trajectories and velocity laws along the path. Future work will include routines for optimization of controller parameters, as well as comparison of different control strategies for the given task.

Acknowledgment. Authors gratefully acknowledge the support of Ministry of Education, Science and Technological Development of the Republic of Serbia under the contract 451-03-47/2023-01/200105 from 03.02.2023 (Projects TR 33047 (P.D.M), TR 35006, III 41006 (M.P.L.)), and 451-03-47/2023-01/200103 (T.B.Š.)

References

[1] B. Siciliano, L. Sciavicco, L. Villani, G. Oriolo, *Robotics*, London: Springer-Verlag, 2009.

[2] H. G. Sage, M. F. De Mathelin, E. Ostertag, "Robust control of robot manipulators: A survey," *Inter J Control*, vol. 76, no. 16, pp. 1498-1522, 1999.

[3] G.K. McMillan, *Industrial applications of PID control*. In: Vilanova R, Visioli A, eds. PID control in the third millenium. London: Springer, pp. 415-461, 2012.

[4] Astrom, K. J., & Hagglund, T. (2006). *Advanced PID control*. The Instrumentation Systems and Automation Society, 2006.

[5] T.B. Šekara, M.R. Mataušek, *Optimization of PID Controller Based on Maximization of the Proportional Gain Under Constraints on Robustness and Sensitivity to Measurement Noise*, IEEE Trans Automat Contr, vol. 54, pp. 184-189, 2009.

[6] Šekara, T. B., & Mataušek, M. R. (2010). *Revisiting the Ziegler-Nichols process dynamics characterization*. Journal of Process Control, 20(3), 360–363.

[7] Šekara, T. B., & Mataušek, M. R. (2011). *Classification of dynamic processes and PID controller tuning in a parameter plane*. Journal of Process Control, 21(4), 620–626.

[8] Mataušek, M. R., & Šekara, T. B. (2011). *PID controller frequency-domain tuning for stable, integrating and unstable processes, including dead-time*. Journal of Process Control, 21(1), 17–27.

[9] P. D. Mandić, M. Č. Bošković, T. B. Šekara, M. P. Lazarević, *A new optimisation method of PIDC controller under constraints on robustness and sensitivity to measurement noise using amplitude optimum principle*, International Journal of Control. doi.org/10.1080/00207179.2021.1912392

[10] A. Kuperman, *Proportional-Resonant Current Controllers Design Based on Desired Transient Performance*, in IEEE Transactions on Power Electronics, vol. 30, no. 10, pp. 5341-5345, Oct. 2015, doi: 10.1109/TPEL.2015.2408053

[11] Đ. M. Stojić and T. B. Šekara, *Digital Resonant Current Controller for LCL-Filtered Inverter Based on Modified Current Sampling and Delay Modeling*, in IEEE Journal of Emerging and Selected Topics in Power Electronics, vol. 10, no. 6, pp. 7109-7119, Dec. 2022.

[12] M. -C. Chou and C. -M. Liaw, *Development of Robust Current 2-DOF Controllers for a Permanent Magnet Synchronous Motor Drive With Reaction Wheel Load*, in *IEEE Transactions on Power Electronics*, vol. 24, no. 5, pp. 1304-1320, May 2009.

[13] Đ. M. Stojić and T. B. Šekara, *A new digital resonant current controller for AC power converters based on the advanced Z-transform*, ISA Transactions, Vol. 129 (part B), pp. 535-545, 2022

[14] J. Wittenburg, Dynamics of Multibody Systems, Springer Verlag Berlin Heidelberg, 2008.

[15] V. Čović, M. P. Lazarević, *Robot Mechanics*, Faculty of Mechanical Engineering, Belgrade, Serbia, 2009.

[16] P. D. Mandić, M. P. Lazarević, Z. Stokić, T. B. Šekara, M., *Dynamic Modelling and Control Design of Seven Degrees of Freedom Robotic Arm,* 6th International Congress of Serbian Society of Mechanics, Tara, Serbia, June 19-21, 2017.

[17] F. L. Lewis, D. M. Dawson, C. T. Abdallah, Robot Manipulator Control, Marcel Dekker, New York, 2004.

[18] P. D. Mandić, M. P. Lazarević, T. B. Šekara, M. Č. Bošković, G. Maione, *Robust control of robot manipulators using fractional order lag compensator,* 7th International Congress of Serbian Society of Mechanics, Sr. Karlovci, Serbia, June 24-26, 2019.

[19] P. D. Mandić, Advanced modeling of complex robotic systems and mechanisms and applications of modern control theory, PhD Dissertation, Faculty of Mechanical Engineering, 2019.

[20] P. D. Mandić, M. P. Lazarević, *An Application Example of Webots in Solving Control Tasks of Robotic System*, FME Transactions (41), pp. 153-162, 2013.

[21] M. Č. Bošković, M. R. Rapaić, T. B. Šekara, P. D. Mandić, M. P. Lazarević, *A novel method for design of complex compensators in control systems,* 18th International Symposium INFOTEH-JAHORINA, March 20-22, 2019.

[22] K. J. Åström, R. M. Murray, *Feedback Systems- An Introduction for Scientists and Engineers*, Princeton, USA: Princeton University Press, 2008.

[23] K. J. Åström, R. H. Panagopoulos, T. Hägglund, *Design of PI Controllers based on Non-Convex Optimization*, Automatica 34(5), pp. 585-601.

[24] M. P. Lazarević, P. D. Mandić, S. Ostojić, *Further results on advanced robust iterative learning control and modeling of robotic systems*, Proc IMechE Part C: J Mechanical Engineering Science, pp. 1-16, 2020.